

Investigation of Structural, Magnetic and Dielectric Properties of Terbium Doped Strontium Hexaferrite for High Frequency Applications

Shivani Malhotra^{1*}, Mansi Chitkara², Inderjeet Singh Sandhu², Naini Dawar¹
and Jaspreet Singh¹

¹School of Electronics and Electrical Engineering, Chitkara University, Rajpura - 140401, Punjab, India; shivani.malhotra@chitkara.edu.in, naini.dawar@chitkara.edu.in, jaspreet.singh@chitkara.edu.in

²Nanomaterial Research Laboratory, Chitkara University, Rajpura - 140401, Punjab, India; mansi@chitkara.edu.in, is.sandhu@chitkara.edu.in

Abstract

Background/Objectives: Microwave absorbing materials can be used to reduce electro-magnetic interference. M-type hexaferrites (SrFe₁₂O₁₉ and BaFe₁₂O₁₉) have attracted intensive attention on account of their important applications in microwave absorbing materials. **Methods/Statistical Analysis:** M-type hexaferrite nanoparticles with a composition of Tb_xSr_{1-x}Fe₁₂O₁₉ (x = 0–0.1) were amalgamated by a chemical method known as co-precipitation method. A successive solid state reaction at different calcination temperatures at fixed holding time has lead to the formation of pure and Tb substituted strontium hexaferrite. The reaction of swapping of Tb cations on the magnetic, structural, and electrical properties of nanoparticles was characterized by X-ray diffraction XRD, FTIR, TEM and VSM. **Findings:** Microstructure by TEM showed that grains are of extremely fine phase. Identification by XRD confers the single-phase material of nanometric size. Evaluation on magnetic characteristics for the material showed that coercivity decreased progressively with substitution of Tb³⁺ ion. Although this was followed by a significant increase in total magnetization. Reflection loss and reflection coefficient and loss tangent for a range of 1-5 KHz were derived which confirms that the material can be considered for high frequency applications.

Keywords: Dielectric Properties, Hexaferrites, Microwave Absorbers, Reflection Loss

1. Introduction

Nano materials have gained popularity in different areas from basic research to various applications in the field of sensors, communication, electronics and radar absorbing materials^{1,2}. Many researchers proposed that many unique properties would emerge from nano sized materials^{3,4}. Therefore the synthesis of these materials is intensively pursued for their fundamental properties, scientific and technological importance. Strontium hexaferrite is considered to be a scientifically favorable material for technological operations in the field of nanoscience

devices. Its high magnetic anisotropy, electrical resistivity, chemical stability and corrosion resistance makes it more suitable to be used as ferrites⁵. Numerous materials have been used as dopant in strontium hexaferrite in order to enhance the electronic and magnetic characteristics of the ferrite⁶⁻⁸. The synthesis of rare-earth Substitute hexaferrite is still a challenge and characteristics of such material required to be analyzed potentially. Microwave Absorbers are the materials that alternate the energy of an electromagnetic wave. These materials are used to eliminate the unwanted radiation that can interfere with the system operation and thus hinder the performance of these systems. Since decade microwave absorber has

*Author for correspondence

been used in military application, for EMI reduction, antenna pattern shaping and radar cross radiation⁹. With the advancement in wireless electronics, a need was felt for material that can absorb the noise at high frequencies¹⁰. Electronic devices operating at high frequency faces a problem with emission of high frequency noise. The radiation emitted in a high-frequency circuit or system are not easy to control. So, in order to overcome this problem RF microwave absorbers are incorporated in circuit to suppress unwanted radiation either from the circuit or outside it. Conventional microwave ferrites do not work well in Giga hertz range because of their high anisotropic field i.e HA. But research has shown that HA of hexagonal ferrites can be improved by trading of rare earth ions like La³⁺¹¹, Eu³⁺¹², Pr³⁺ etc. Though Several techniques have been evolved to synthesize Sr-hexaferrite such hydrothermal method¹³, solgel¹⁴, microwave induced conduction, ball milling¹⁵, chemical co precipitation¹⁶⁻¹⁸. The focus of all these methods still remain the same to attain ultra-fine size of strontium hexaferrite with high level of purity to exhibit required/special magnetic characteristics. The best method is Co-precipitation for the formation of hexaferrite due to its homogeneity, composition while preparation and lower synthesis temperature¹⁹. In the present work for characteristic and synthesis of hexaferrite chemical co-precipitation method is opted. During preparation process other parameters like Fe³⁺/Sr²⁺ molar ratio, calcination temperature and pH level can also be controlled in order to get desired product^{9,16}. Further structural, magnetic and dielectric properties are explored on substitution of Tb³⁺ ions at strontium sites. Such kind of study is intended to provide facilitation for designing of microwave devices.

2. Experimental Procedure

2.1 Synthesis

The method of preparation performs a crucial player in finding the characteristics of terbium doped strontium hexaferrite. In the present work the method opted is chemical co-precipitation method to synthesize ferrite composition having formula $Tb_xSr_{1-x}Fe_{12}O_{19}$ with $x = 0.02, 0.04, 0.06, 0.08$ and 0.10 . Terbium doped strontium hexaferrite was prepared at Nano Material Research Laboratory of Chitkara University. All the precursors

were of analytical grade chlorides. Calculated amount of salts of Ferric Chloride (FeCl₃), Terbium Chloride (TbCl₃) and Strontium Chloride (SrCl₂) were dissolved in deionised water and stirred for 1 hour. 10M NaOH solution was then slowly added drop wise to the mixture under rigorous stirring. The alkali addition was continued till the PH value of the solution was achieved 12 and was left undisturbed for few hours for complete digestion. The brownish precipitates of metal hydroxides appeared as the PH of value 12 is achieved. The precipitates were filtered and washed repeatedly with water and lastly with alcohol. They were then dried in hot air oven (Universal itherm A1-7981) at a temperature of 100^o C.

The obtained sample was then grinded into fine powder. The entire process was repeated for series of samples where x varies as 0.02, 0.04, 0.06, 0.08 and 0.10 and is heat treated at 850^o C for 4 hours in muffle furnace (Navyug indiaNIC-4000). The strontium hexaferrite formation was proved from Fourier Transform Infrared Spectroscopy. Using using X-Ray diffractometer (XPRT-PRO PW 3050/60) the analysis of structure was done with CuK α radiations and the magnetic characteristics were systematically studied from VSM results and electrical properties were also investigated using a two probe method.

3. Results and Discussion

3.1 FTIR (Fourier Transform Infrared Spectroscopy)

FTIR spectra of pure strontium hexaferrite samples and terbium doped strontium hexaferrite sample was accomplished for a range of 400-4000 cm⁻¹. Potassium bromide powder was mixed with strontium ferrite powder for pelletisation of the sample. Perkin Elmer-USD FTIR spectrometer was used to record FTIR spectra of pure and doped samples.

It was observed from Figure 1 and Figure 2 that there is a decrease in the transmittance of hexaferrite powder because of the absorption of fringing field by the powder. The FTIR spectra of strontium hexaferrite powders shown in fig 1 shows three significant transmittance peaks of hexaferrite at ~ 408 cm⁻¹, 481cm⁻¹ and 545cm⁻¹ which are in sync with finding of other researchers²⁰. The results in Figure 2 showed that transmittance peaks

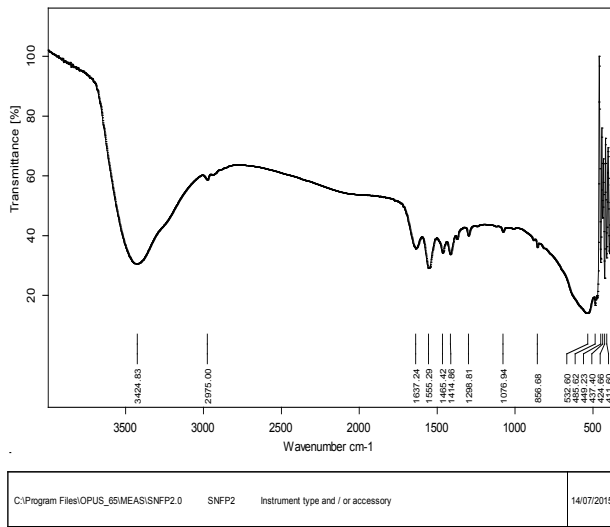


Figure 1. FTIR-spectrum of pure strontium hexaferrite powder.

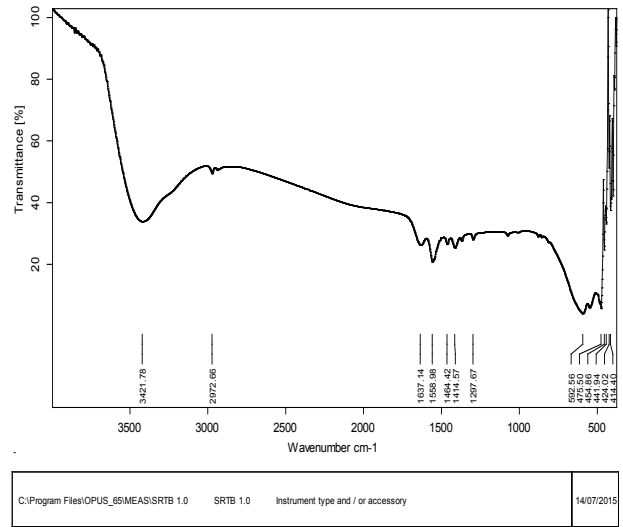


Figure 2. FTIR-spectrum of terbium doped strontium hexaferrite powder.

decreases with the substitution of Tb³⁺ in the SrM thus conferring absorption.

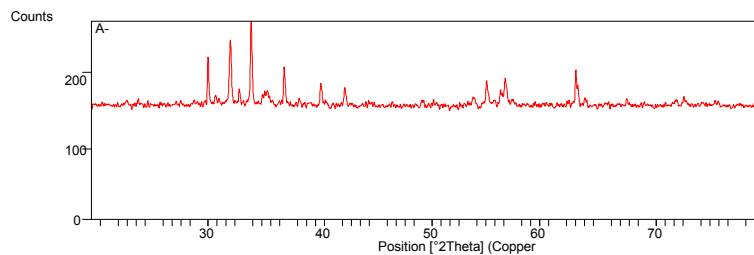
3.2 X-Ray Diffraction Analysis

Patterns of calcined powder are shown in Figure 3(a) and Figure 3(b). It is observed that the sample consist of pure strontium ferrite phase. The peak for both pre and doped ferrite appear at same place with different intensity. In case of doped ferrite with different concentration of Tb (x = 0.02, 0.04, 0.06, 0.08, 0.10) rearranged in hexagonal structure. Structural analysis and identification of phase was carried out on PAN analytical X-ray (X-PERT PRO)

which has (λ) = 1.54 Å for CuK α . The scan rate of the machine was 0.0170°/sec. The scattering angle range (2θ) was chosen to be varying from 20° to 80°. The specimen length was taken 10 mm. The broadening of the X-ray line helped in determining the particle size d. Scherrer’s Equation so used to calculate d is as under:

$$d = K\lambda / \beta \cos\theta \quad (1)$$

In the Equation (1) is full width at half-maximum expressed in units of 2θ and θ is the Bragg angle λ is the wavelength of X-rays, k (shape factor) is taken ~ 0.9. The pattern produced showed the presence of SrFe₁₂O₁₉. JCPDS data as mentioned in the literature is being com-



(a)

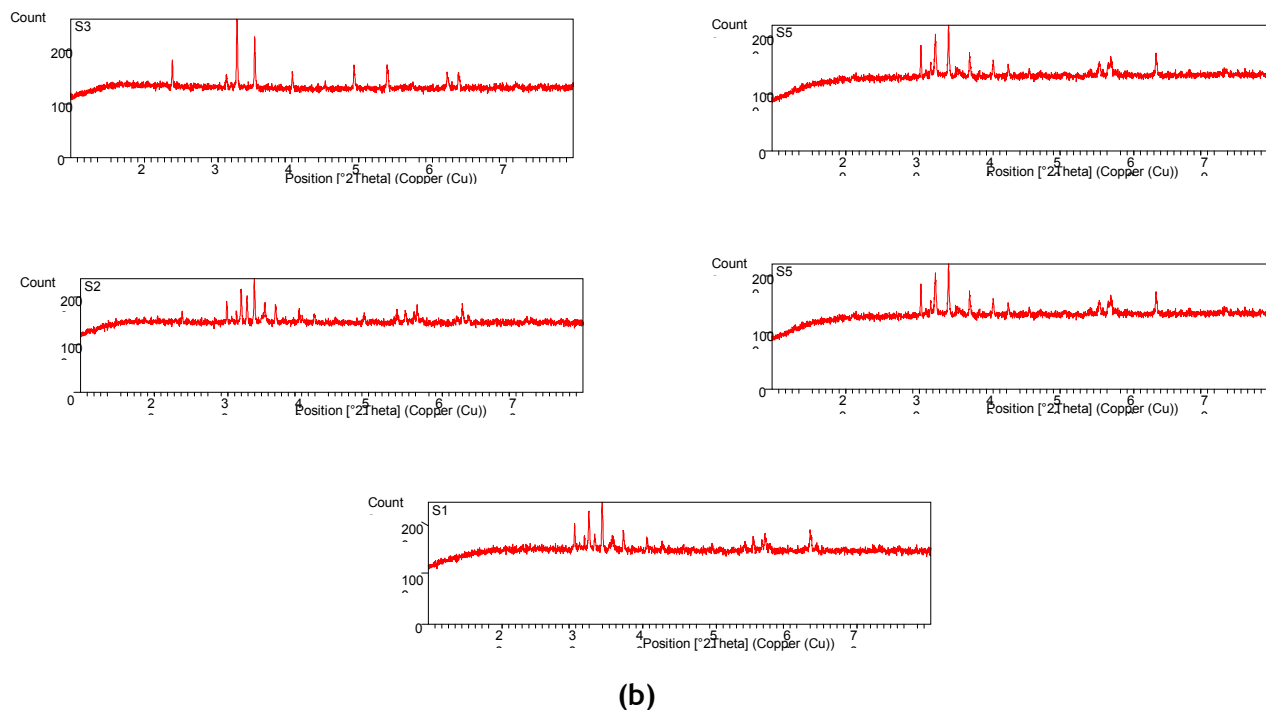


Figure 3. (a) XRD Pattern For pure strontium hexaferrite calcined at 850° C for 4 hrs. (b) XRD Pattern for terbium doped strontium hexaferrite for (x= 0.02, 0.04, 0.06, 0.08, 0.10) calcined at 850° C for 4 hrs.

Table 1. XRD analysis with increase in concentration of terbium doping

X(dopant concentration)	Typical peaks 2θ	D spacing(Å)	Crystallite size D nm
0	35.8326	2.5007	49
0.02	32.3579	.0836	90
0.04	32.1892	2.6226	83
0.06	31.7057	2.8221	64
0.08	33.145	2.7081	58
0.10	34.5877	2.5937	52

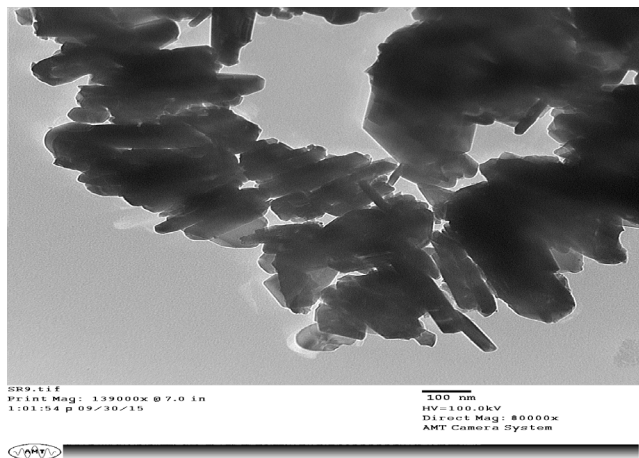
pared with all the identified peaks. JCPDS 84-1531²¹ was used for reference and indexing.

It has been observed that without calcination the particles are in amorphous form; however on calcination they get crystallite size as indicated in the results. The pattern shows peak formation and broadening after substituting different concentration of terbium in strontium hexaferrite sample. The average size of crystallite for major peaks as measured using the Scherer Equation (1) lies between 40–90 nm.

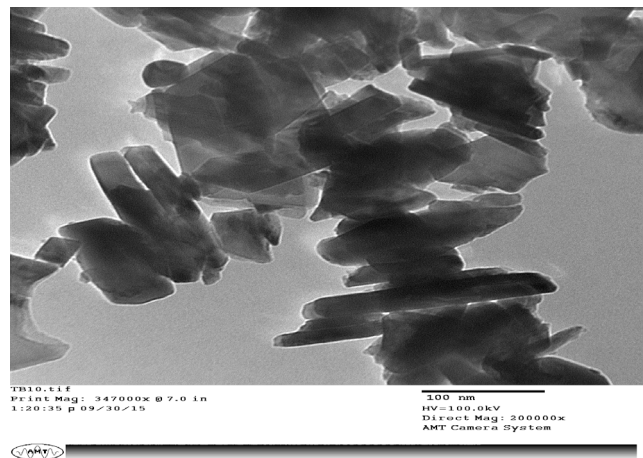
It is revealed from the graph that the crystallite size for the produced ferrite decreased with an increase in dopant concentration. Same is also shown in the form of a Table 1 given above. Thus we can say that terbium acts as a grain growth inhibitor.

3.3 Transmission Electron Microscopy (TEM)

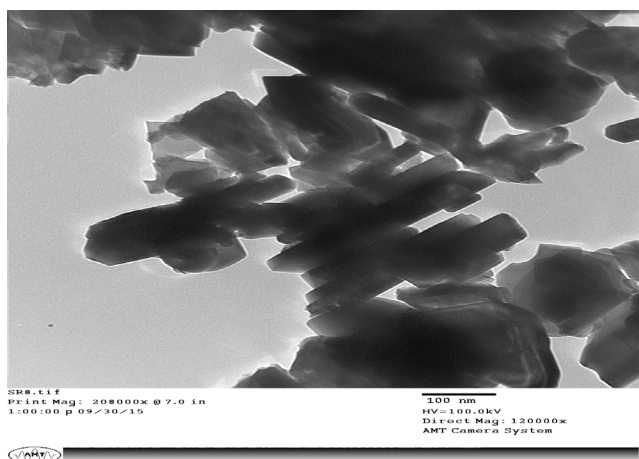
Terbium doped strontium hexaferrite have large surface to volume ratio due to their large surface area. This results in high agglomeration of ferrite particles. Therefore, in order to obtain TEM images the strontium hexaferrite particles were first ultrasonically agitated. The micrographs of $\text{SrFe}_{12}\text{O}_{19}$ and $\text{Tb}_{0.1}\text{Sr}_{0.9}\text{Fe}_{12}\text{O}_{19}$ were recorded and then investigated. These micrographs as shown in Figure 4 reveals that particles with mean size 2 nm-120 nm had typical hexagonal and plate like morphology. The particle size increases due to addition of dopant. The phase formation of the particle depends on the homogeneous distribution of the metal ions in the co-precipitated pre-



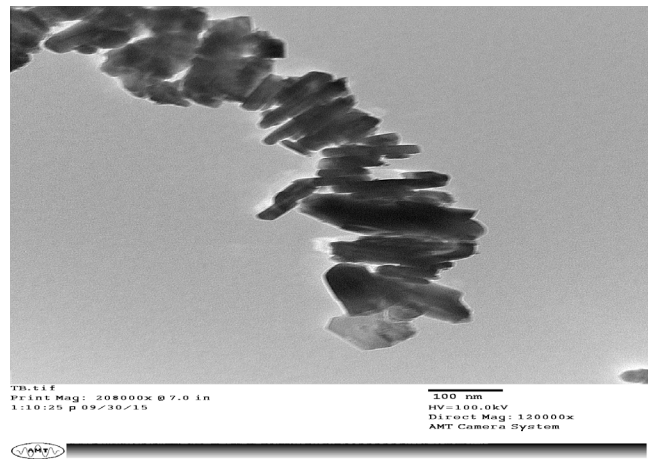
(a)



(c)



(b)



(d)

Figure 4. TEM micrographs pure Strontium hexaferrite (a)(b) Terbium doped (c)(d) Synthesized samples calcined at 8000C.

cursors used and on subsequent calcination temperature. Further the particle size and morphology of the synthesized powder depends on the nucleation and growth of particle. As seen in micrographs the particles were agglomerated due to addition of interfacial surface tension²².

3.4 Magnetic Properties

A VSM (Vibrating Sample Magnetometer) under the applied field of 15 KOe was used to determine and analyse the magnetic properties of SrFe₁₂O₁₉ particle and Tb_xSr_{1-x}Fe₁₂O₁₉ particles. The hysteresis loop result from VSM studies provides the relation between Magnetization (M) and applied field (H) at room temperature. The parameter extracted from the loop are saturation Coercivity (Hc), Magnetization (Ms), and remanence (Mr). Figure 6 and Figure 7 shows the hysteresis loop for SrFe₁₂O₁₉ and Tb_xSr_{1-x}Fe₁₂O₁₉. High value of Hc 5126KOe and 4896KOe for pure and doped strontium hexaferrite respectively confirm it as a hard magnetic material. At room temperature with the help of alkaline metal chloride salt, Nanonocrystalline Sr-hexaferrite can be made. At 600° C, material was amorphous, with Ms = 3.3 Am²Kg⁻¹ and Hc of the order of 5KOe but by 850 it has crystallized and Ms has risen to 24.3emu/g which further increased to 42.6 emu/g on addition of terbium as a dopant.

The magnetron number n_B is obtained using relation:

$$n_B = (\text{molecular weight} * Ms) / 5585 \quad (2)$$

where Ms is the saturation magnetization of the segment²³. The values of magnetron number are mentioned in Table 4. The values of magnetron number increases on exchanging of Tb ion and this is somewhere related to the increased magnetization of the sample on substitution of the dopant. The squareness ratio (Mr/Ms)>0.5 signify formation of single magnetic domain and that with < 0.5 leads to multidomain structure²⁴. So, it is evident from the results as shown in Table 2 that single magnetic domain is present in both pure as well as terbium doped stron-

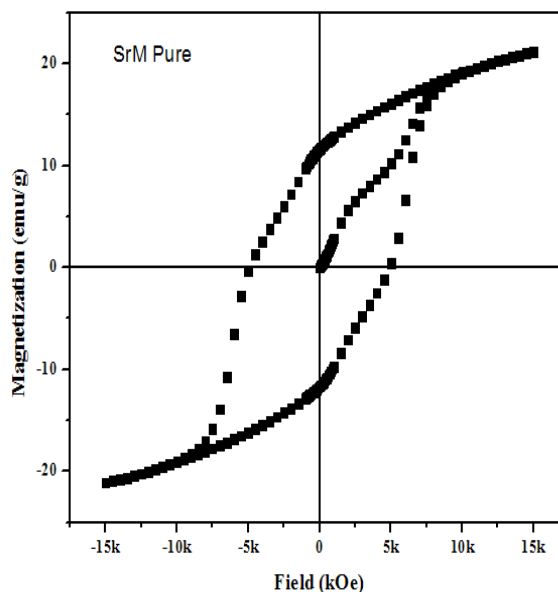


Figure 6. Hysteresis plot of SrFe₁₂O₁₉ nanoferrites calcined at 850°C.

Table 2. Magnetic characteristics of pure and terbium doped strontium hexaferrite

Samples	Ms (emu/g)	Mr (emu/g)	Mr/Ms	Hc(KOe)	n_B
SrFe ₁₂ O ₁₉	24.3	13.2	.5432	4.826	4.62
Tb _{0.1} Sr _{0.9} Fe ₁₂ O ₁₉	42.6	22.4	.5258	5.126	8.15

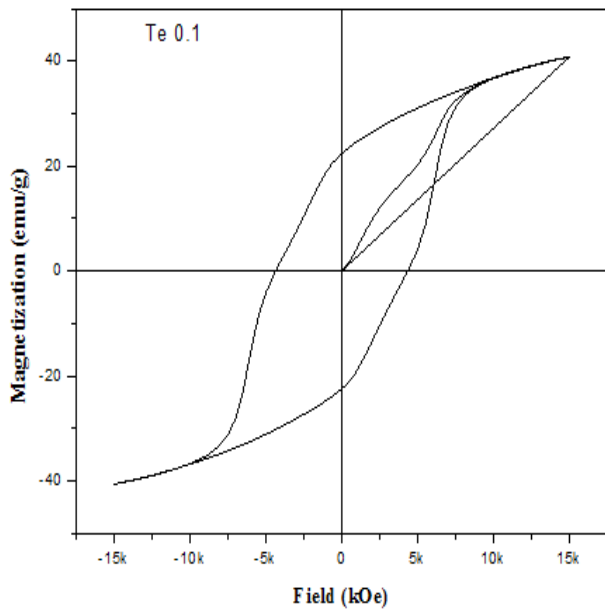


Figure 7. Hysteresis plot of $Tb_xSr_{1-x}Fe_{12}O_{19}$ nanoferrites calcined at $850^{\circ}C$.

tium hexaferrite. Coercivity is an extrinsic property of a material that can be controlled by regulating the crystallite shape, size and distribution of the size²⁵. If $H_c > Mr/2$ the material are strong material and are useful in high frequency application. In this work the values of the magnetic parameters investigated is in sync with the above mentioned equation. Therefore pure and terbium doped strontium hexaferrite are useful at high frequency applications.

3.5 Dielectric Characterization

The dielectric properties were measured using a two probe method. In this method a fixture was created to test the electrical properties of the sample for a frequency range of 1Hz –5KHz. The test fixture was adjusted to act like a parallel plate in order to determine the electrical permittivity and loss tangent of pure and doped materials the schematic is shown in Figure 8(a) and Figure 8(b).

In this method the sample to be tested is placed between two rectangular plates to create a unit just like parallel plate capacitor. With this setup an LCR meter was used to determine the value of load. Which is mathematically described below:

$$\tan \delta = \epsilon''/\epsilon' \quad \text{-----(3)}$$

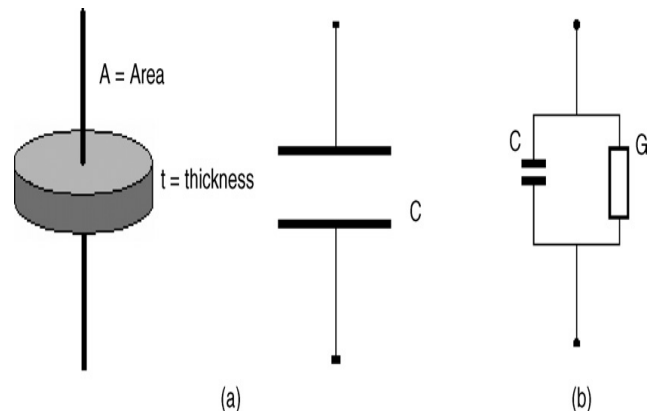


Figure 8. (a) Parallel plate arrangement for dielectric characteristics measurement (b) Equivalent circuit.

Co-precipitation methods prepared by chemical dielectric properties of the $SrFe_{12}O_{19}$ hexaferrite are shown in Figures 9–12. All the statistics are recorded in a scale of 1 Hz–5 kHz at an ambient temperature. Graphs in the figs. below are in accordance to the assumption made theoretically that, when any dielectric material is exposed to an ac electric field a delay is seen as well as loss in the dielectric response with the field.

Real part ($\epsilon' r$) signifies the quantity of energy stored in the dielectric material from the ac field whereas the imaginary part ($\epsilon'' r$) signifies the loss to the ac electric field. Thus, the loss tangent, $\tan \delta$ is the ratio of the imaginary part to the real part of the complex relative permittivity. As the frequency increases, loss tangent and dielectric decreases which can be noticed from the result. The dielectric loss tangent for strontium is almost approaching zero which reveals that strontium ferrite is a sort of non-dielectric absorbing material. The dielectric loss tangent of terbium doped strontium ferrite decreases in comparison to pure strontium ferrite. This confirms improved dielectric reported on addition of dopant.

The dielectric loss tangent of terbium doped strontium is increasing in comparison to pure doped strontium hexaferrite. This acknowledges improved dielectric properties on addition of dopants. The electron reaches the grain boundary by a phenomenon of hopping. These electrons remain piled up there if the resistance of grain boundary is high and thus leads to polarization. A space charge carrier needs some finite time to align their axis

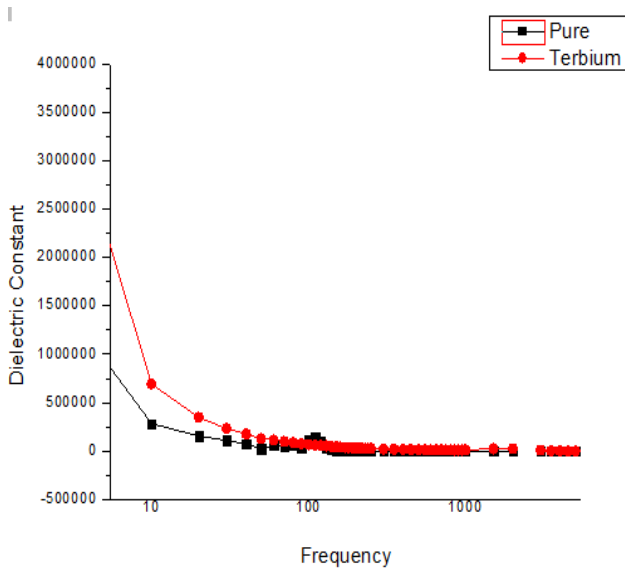


Figure 9. Variation of dielectric constant with applied field frequency.

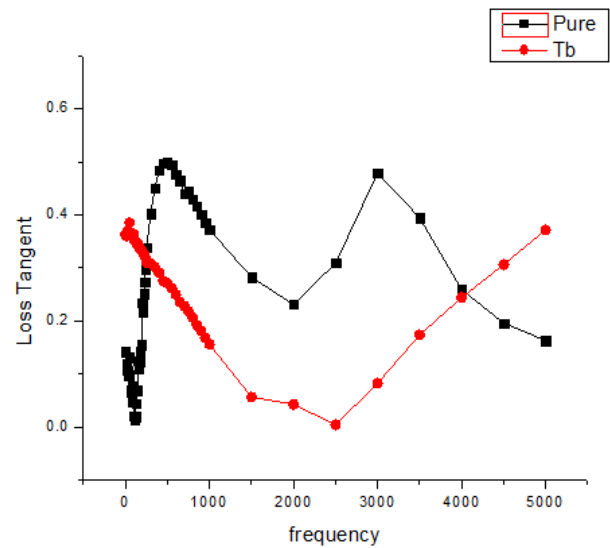


Figure 11. Variation of loss tangent with applied field frequency.

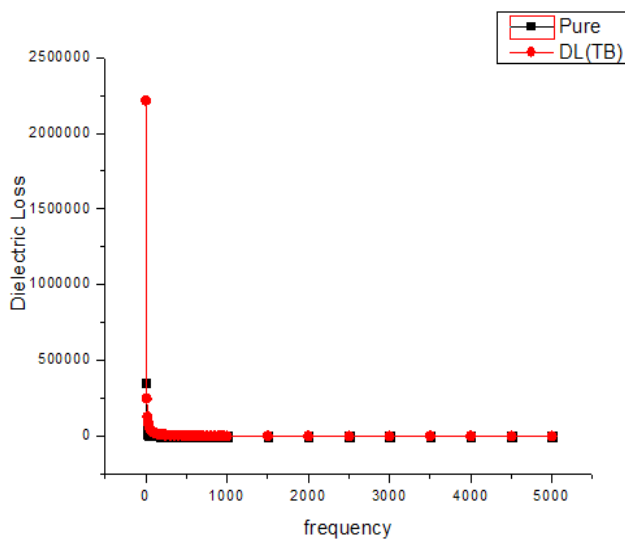


Figure 10. Variation of dielectric loss with applied field frequency.

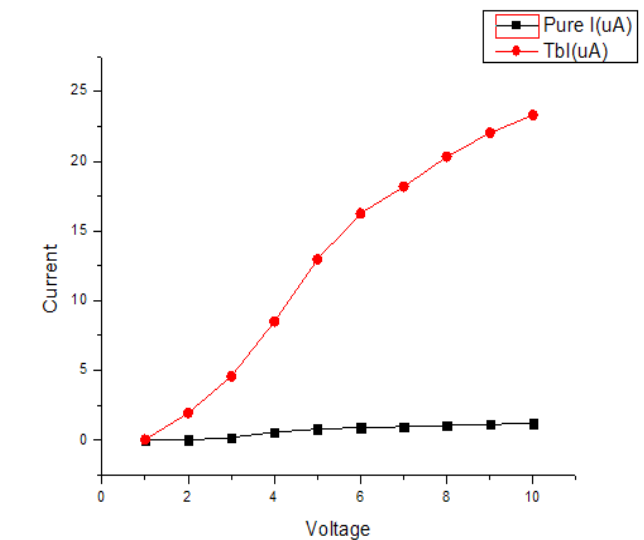


Figure 12. Variation of ac conductivity with applied field frequency.

to in the direction of applied ac field. As pure strontium hexaferrite sample is exposed to increased frequency the carrier are required to align their axis to the applied ac field more frequently. Thus reducing their possibility to reach to grain boundary which in turn leads to reduced polarization. The low dielectric loss tangent value for both pure and doped strontium hexaferrite also confirms more

perfect structure homogeneity. Acelectrical conductivity becomes more linear on addition of dopant. Its linearity confirms polar on type conduction. It is evident from the results shown by the graphs in Figure 9, 10 that dielectric loss and dielectric constant are decreasing with the increase in frequency.

4. Conclusion

In this study the Nano-crystalline samples of $\text{SrFe}_{12}\text{O}_{19}$ and $\text{Tb}_x\text{Sr}_{1-x}\text{Fe}_{12}\text{O}_{19}$ with $x = 0.02, 0.04, 0.06, 0.08$ and 0.10 were obtained by chemical co-precipitation method. The prepared samples exhibited a hexagonal structure with size varying from 40 nm–90 nm. The XRD pattern obtained showed some extra phase on addition of terbium but overall pattern confirmed the hexagonal structure with a high degree of crystallinity. The morphology of the samples consists of the rain with relatively homogeneous distribution as seen by TEM micrographs. The substitution of Tb ions caused appreciable changes in the structural and magnetic properties of strontium hexaferrite. Increase in the value of coercivity on addition of terbium confirms it as a hard magnetic material. The present study confirms the presence of single magnetic domain as the squareness ratio is less than 0.5. The result showed that dielectric constant and dielectric loss decreases with increase in frequency which was explained by Maxwell–Wager theory. AC conductivity showed an improvement with increase in frequency in case of terbium doped strontium hexaferrite when compared with pure form.

5. References

1. Pullar RC. Hexagonal ferrites: A review of the scope indexed journal magnetic material synthesis, properties and applications of hexaferrite. *Ceramics Journal on Progress in Materials Science*. 2012; 57:1191–334.
2. Smit J, Wijn HPJ. *Ferrites*. New York: Philip's Tech. Library; 1959.
3. Gordani GR, Ghasemi A, Saidi A. High frequency electromagnetic reflection loss performance of substituted Sr-hexaferrite nanoparticles/SWCNTs/epoxy nanocomposite. *Journal of Magnetism and Magnetic Materials*. 2015; 391.
4. Afsar MN, Sharma A, Obol M. Microwave permittivity and permeability properties and microwave reflection of micro/nano ferrite powder. *Proceedings of IEEE Conference Instrumentation and Measurement Technology*; 2009. p. 274-8.
5. Ghoutia, Naima, Sabri. Nonreciprocal propagation in ferrite medium and their applications microwave circulator. *International Journal of Computer Science and Electronics Engineering*. 2013; 1(2):2320–34.
6. Caffarena VR, Capitaneob JL, Ogasawarac T, Pinhod MS. Microwave absorption properties of Co, Cu, Zn - substituted hexaferrite polychloroprene nanocomposites. *Materials Research*. 2008; 11(3):335-9.
7. Doni R, Manaf A, Sardjono P. Physical characteristics and magnetic properties of Barium Hexaferrites ($\text{BaFe}_{12}\text{O}_{19}$) derived from mechanical alloying. *International Journal of Basic and Applied Sciences*. 2008; 13(4).
8. Sharbati A, Khani JMV, Amiri GR, Mousarezaei R. Influence of dysprosium addition on the structural, morphological, electrical and magnetic properties of nano-crystalline W-type hexaferrites. *Bulletin of Materials Science*. 2011; 38(1):1-5.
9. Wang Y, Li T, Zhao L, Hu Z, Gu Y. Research Progress on nanostructured radar absorbing materials. *Journal on Energy and Power Engineering*. 2011; 3:580-4.
10. Shigeyoshi Y, Koichi K, Hiroshi O. High-frequency noise suppression using ferrite-plated film. *NEC Technical Journal*. 2009; 1(5):77-81.
11. Luo H, Rai BK, Mishra SR, Nguyen VV, Liu JP. Physical and magnetic properties of highly aluminum doped strontium ferrite nanoparticles prepared by auto-combustion route. *Journal of Magnetism and Magnetic Materials*. 2012; 324(17):2602–8.
12. Y xie, XW hong, YH GaO, JM Liu. Synthesis and electromagnetic properties of $\text{BaFe}_{11.92}(\text{LaNd})_{0.04}\text{O}_{19}$ /titanium dioxide composites. *Materials Research Bulletin*. 2014; 50, 483–489.
13. Xie Y, Hong X, Liu J, Le Z, Huang F, Qin Y, Zhong R, Gao Y, Pan J, Ling Y. Synthesis and electromagnetic properties of $\text{BaFe}_{11.92}(\text{LaNd})_{0.04}\text{O}_{19}$ /titanium dioxide composites. *Materials Research Bulletin*. 2014; 50:483–9.
14. Ghobeiti-Hasab M, Shariati Z. Magnetic properties of Sr-Ferrite Nano-Powder synthesized by Sol-Gel auto-combustion method. *International Journal of Chemical, Nuclear, Metallurgical and Materials Engineering*. 2014; 8(10):954-7.
15. Jean M, Nachbaur V, Bran J, Breton JM. Synthesis and characterization of $\text{SrFe}_{12}\text{O}_{19}$ powder obtained by hydrothermal process. *Journal of Alloys and Compounds*. 2010; 480:306–12.
16. Kumar K, Chitkara M, Sandhu IS, Mehta D, Kumar S. Photocatalytic, optical and magnetic properties of Fe-doped ZnO nanoparticles prepared by chemical route. *Journal of Alloys and Compounds*. 2014; 588:681-9.
17. Chitkara M, Singh K, Sandhu IS, Bhatti HS. Photo-catalytic activity of $\text{Zn}_{1-x}\text{Mn}_x\text{S}$ nanocrystals synthesized by wet chemical technique. *Nanoscale Research Letters*. 2011; 6(1):1-5.

18. Ibrahim RM. A novel approach for synthesise of M-type hexaferrite nanopowder via the co-precipitation method. *Springer Journal of Materials Science: Materials in Electronics*. 2011; 22(12):1796-1803.
19. Petcharoen K, Sirivat A. Synthesis and characterization of magnetite nanoparticles via the chemical co-precipitation method. *Journal of Materials Science and Engineerig*. 2012; 177(5):421-7.
20. Mangai A, Kumari PR, Kumar S. Spectroscopic investigation of nano-sized strontium ferrite particles at different annealing temperatures. *Journal of Applied Spectroscopy*. 2014; 81(3).
21. Silva WMS, Ferreira NS, Soares JM, Silva RB, Macedo MA. Investigation of structural and magnetic properties of nanocrystalline Mn-doped SrFe₁₂O₁₉ prepared by proteic sol-gel process. *Journal of Magnetism and Magnetic Materials*. 2015; 395:263-70.
22. Osman MA, Atallah A, Schweizer T, Ottinger HC. Particle-particle and particle-matrix interactions in calcite filled high-density polyethylene-steady shear. *Journal of Rheolog*. 2004; 48:1167-84.
23. Verma S, Chand J, Singh M. Mossbauer, magnetic, dielectric and dc conductivity of Al³⁺ ions substituted Mg-Mn-Ni nano ferrite synthesized by citrate precursor method. *Advanced Material Letter*. 2013; 4(4):310-6.
24. Mangai KA, Sureshkumar P, Priya M, Rathnakumar M. Structural and magnetic properties of strontium hexaferrites for permanent magnets. *International Journal of Scientific and Engineering Research*. 2014; 5:3.
25. Ali I, Islam MU, Awan MS, Ahmad M, Iqbal MA. Structural and magnetic properties of nano-structured Eu³⁺Substituted M-type hexaferrites synthesized by Sol-Gel auto-combustion technique. *Journal of Superconductivity and Novel Magnetism*. 2013; 26:3315-23.